

# Age-Dependent Changes in Heparan Sulfate in Human Bruch's Membrane: Implications for Age-Related Macular Degeneration

Tiarnan D. L. Keenan,<sup>1-4</sup> Claire E. Pickford,<sup>5</sup> Rebecca J. Holley,<sup>4,5</sup> Simon J. Clark,<sup>1,2</sup> Wanchang Lin,<sup>2,6</sup> Andrew W. Dowsey,<sup>2,6</sup> Catherine L. Merry,<sup>5</sup> Anthony J. Day,<sup>4</sup> and Paul N. Bishop<sup>1-3</sup>

<sup>1</sup>Centre for Hearing & Vision Research, Institute of Human Development, University of Manchester, Manchester, United Kingdom

<sup>2</sup>Centre for Advanced Discovery and Experimental Therapeutics (CADET), University of Manchester and Central Manchester University Hospitals NHS Foundation Trust, Manchester Academic Health Science Centre, Manchester, United Kingdom

<sup>3</sup>Manchester Royal Eye Hospital, Central Manchester University Hospitals NHS Foundation Trust, United Kingdom

<sup>4</sup>Wellcome Trust Centre for Cell-Matrix Research, Faculty of Life Sciences, University of Manchester, Manchester, United Kingdom

<sup>5</sup>Stem Cell Glycobiology, School of Materials, University of Manchester, Manchester, United Kingdom

<sup>6</sup>Centre for Endocrinology and Diabetes, Institute of Human Development, University of Manchester, Manchester, United Kingdom

Correspondence: Paul N. Bishop, Institute of Human Development, AV Hill Building, University of Manchester, Oxford Road, Manchester M13 9PT, UK; paul.bishop@manchester.ac.uk.

Anthony J. Day, Faculty of Life Sciences, Michael Smith Building, University of Manchester, Oxford Road, Manchester M13 9PT, UK; anthony.day@manchester.ac.uk.

Submitted: February 24, 2014

Accepted: July 10, 2014

Citation: Keenan TDL, Pickford CE, Holley RJ, et al. Age-dependent changes in heparan sulfate in human Bruch's membrane: implications for age-related macular degeneration. *Invest Ophthalmol Vis Sci*. 2014;55:5370-5379. DOI:10.1167/iovs.14-14126

**PURPOSE.** Heparan sulfate (HS) has been implicated in age-related macular degeneration (AMD), since it is the major binding partner for complement factor H (CFH) in human Bruch's membrane (BrM), and CFH has a central role in inhibiting complement activation on extracellular matrices. The aim was to investigate potential aging changes in HS quantity and composition in human BrM.

**METHODS.** Postmortem human ocular tissue was obtained from donors without known retinal disease. The HS was purified from BrM and neurosensory retina, and after digestion to disaccharides, fluorescently labeled and analyzed by reverse-phase HPLC. The HS and heparanase-1 were detected by immunohistochemistry in macular tissue sections from young and old donors, and binding of exogenously applied recombinant CCP6-8 region of CFH (402Y and 402H variants) was compared.

**RESULTS.** Disaccharide analysis demonstrated that the mean quantity of HS in BrM was 50% lower ( $P = 0.006$ ) in old versus young donors (average 82 vs. 32 years). In addition, there was a small, but significant decrease in HS sulfation in old BrM. Immunohistochemistry revealed approximately 50% ( $P = 0.02$ ) less HS in macular BrM in old versus young donors, whereas heparanase-1 increased by 24% in old macular BrM ( $P = 0.56$ ). In young donor tissue the AMD-associated 402H CCP6-8 bound relatively poorly to BrM, compared to the 402Y form. In BrM from old donors, this difference was significantly greater ( $P = 0.019$ ).

**CONCLUSIONS.** The quantity of HS decreases substantially with age in human BrM, resulting in fewer binding sites for CFH and especially affecting the ability of the 402H variant of CFH to bind BrM.

**Keywords:** Bruch's membrane, heparan sulfate, AMD

Age-related macular degeneration (AMD) is the leading cause of blindness in developed countries.<sup>1,2</sup> Genetic and biochemical evidence has strongly implicated dysregulation of the complement system in disease pathogenesis.<sup>3-5</sup> Polymorphisms and rare variants in the genes for several different complement components and regulators are associated with increased or decreased AMD risk.<sup>6-12</sup> In particular, the Y402H polymorphism in complement factor H (CFH) has been demonstrated consistently as a common and important risk factor.<sup>6-9,11-13</sup> The disease-associated 402H form is present in approximately 30% of individuals of Caucasian descent, and those homozygous for this allele have over 5-fold increased risk of AMD.<sup>13</sup>

Drusen, the extracellular deposits found in the macular Bruch's membrane (BrM) that are characteristic of early AMD, are known to contain complement components, including

activation products and regulatory proteins.<sup>4,14-16</sup> In addition, the membrane attack complex (MAC) has been observed consistently by immunohistochemistry in human BrM and the choriocapillaris,<sup>6,17-19</sup> and its level was found to increase with age.<sup>20</sup> Importantly, the amount of MAC in human BrM/choroid is significantly higher in individuals who are homozygous for the CFH 402H polymorphism.<sup>21</sup>

A novel potential mechanism linking the Y402H polymorphism and AMD risk was suggested by the finding that the main binding partner of CFH in human macular BrM is heparan sulfate (HS), and that the 402H form of CFH binds poorly to human BrM HS, in comparison with the 402Y form.<sup>22,23</sup> The Y402H polymorphism alters the specificity of CFH for HS such that the 402H variant requires a high level of sulfation for binding.<sup>24,25</sup> The BrM is important in AMD pathogenesis, since this extracellular matrix is a site of drusen formation.<sup>26,27</sup> In

addition, in this acellular environment, CFH is the only negative regulator of the complement alternative pathway, whereby it has a key role in preventing the amplification of complement activation.<sup>3,5</sup>

Heparan sulfate is a member of the glycosaminoglycan (GAG) family of long unbranched polysaccharides, and is composed typically of approximately 50 to 200 repeating disaccharides of glucuronic acid (GlcA) or iduronic acid linked to N-acetylglucosamine (GlcNAc).<sup>5,28,29</sup> The HS chains, as is the case for most other GAGs, are found covalently attached to proteoglycan (PG) core proteins; that is, forming an HSPG.<sup>30,31</sup> In extracellular matrices containing basement membranes, like human BrM, HSPGs include perlecan, agrin, and collagen-XVIII.<sup>32</sup> The variable substitution of sulfate groups at distinct positions within the repeating disaccharide leads to a large number of possible sequence permutations; it is this enormous structural heterogeneity between different HS chains that underpins the great diversity in their biological functions.<sup>5,28,29,33</sup> The HS and HSPGs, which are widely distributed throughout human macular tissue layers,<sup>32,34</sup> are involved in many aspects of cell-matrix interaction and the regulation of inflammation.<sup>35,36</sup> In addition to its role in ocular disease, which recently has been reviewed,<sup>37</sup> HS has been implicated in Alzheimer's disease pathogenesis<sup>38</sup> (which has important parallels with geographic atrophy<sup>39,40</sup>), as well as cancer metastasis and angiogenesis<sup>41,42</sup> (which has similar parallels with choroidal neovascularization).

Previous studies have shown that the 402Y form of CFH can bind to a wide range of HS structures, as demonstrated by in vitro experiments with selectively desulfated heparin preparations.<sup>24,25</sup> By comparison, the AMD-associated 402H form of CFH has a narrow specificity and requires a high degree of sulfation. Therefore, we hypothesized that, if there were an age-related decrease in the amount or sulfation of HS in human BrM, this could contribute to AMD pathogenesis,<sup>3,22,28</sup> with the Y402H polymorphism in combination with age-related changes in HS resulting in decreased CFH binding and failure to regulate complement activation.

In this study, we have characterized/quantitated HS from human BrM and neurosensory retina (NSR) from donors of different age; that is, by reverse-phase HPLC (RP-HPLC) of fluorescently-labeled HS disaccharides. Age-related changes in HS and heparanase-1 were investigated by immunofluorescent microscopy, along with the ability of the CCP6-8 region of CFH to recognize and bind BrM, comparing the 402Y form and the AMD-associated 402H variant.

## METHODS

### HS Extraction

Postmortem human eyes were obtained from the Manchester Eye Bank after removal of the corneas for transplantation. In all cases prior consent had been obtained for the ocular tissue to be used for research, and guidelines established in the Human Tissue Act 2004 were followed. Our research adhered to the tenets of the Declaration of Helsinki. Eyes were from human donors without known retinal disease or visual impairment.

We dissected 34 globes (17 pairs from 17 donors, in two age groups between 26 and 92 years; see Supplementary Table S1) as previously described<sup>32</sup> to obtain the NSR and, separately, isolated BrM. Briefly, the NSR was obtained by gripping it with forceps and cutting it at its point of attachment to the optic disc. The RPE/BrM/choroid tissue complex then was obtained by gentle dissection from the sclera, and isolated BrM obtained by removing the RPE and the choroid through repeated application of a cell scraper to both sides until a homogeneous

gray tissue layer was left. For each donor, the respective tissues were pooled from both eyes. The GAGs then were extracted separately from the BrM and NSR using a previously described method.<sup>43</sup> Briefly, samples were disaggregated mechanically and treated with pronase (7 U [1 mg] per sample, from *Streptomyces griseus*; Roche Diagnostics Ltd, Burgess Hill, UK) in 10 mL of PBS (Oxoid; 137 mM NaCl, 2.6 mM KCl, 8.2 mM Na<sub>2</sub>HPO<sub>4</sub>, 1.5 mM KH<sub>2</sub>PO<sub>4</sub>, pH 7.3) for 4 hours at 37°C. Triton X-100 was added to a final concentration of 1% (vol/vol) for 2 hours at room temperature before a further 7 U of pronase was added for 4 hours at 37°C. Preparations then were loaded onto a 1 mL diethylaminoethanol (DEAE)-Sephacrose Fast Flow (Fisher Scientific UK Ltd., Loughborough, UK) column, pre-equilibrated with 0.15 M NaCl, 20 mM NaH<sub>2</sub>PO<sub>4</sub>·H<sub>2</sub>O (pH 7.0), and washed with 50 mL of 0.25 M NaCl, 20 mM NaH<sub>2</sub>PO<sub>4</sub>·H<sub>2</sub>O (pH 7.0) to remove hyaluronan. The GAGs were eluted with 5 mL of 1.5 M NaCl, 20 mM NaH<sub>2</sub>PO<sub>4</sub>·H<sub>2</sub>O, desalted using a PD10 column (Amersham Biosciences, Little Chalfont, UK), and freeze-dried.

### Preparation and Analysis of 2-Aminoacridone (AMAC)-Labeled Disaccharides

The HS chains in the GAG samples were digested using 5 mIU each of heparinase I, II, and III (from *Flavobacterium heparinum*; Iduron, Manchester, UK) in 100 µL of 0.1 M sodium acetate and 0.1 mM calcium acetate (pH 7.0). The resulting disaccharides then were freeze-dried and redissolved in 10 µL of 0.1 M AMAC in 85% Me<sub>2</sub>SO, 15% acetic acid (vol/vol) and incubated at room temperature for 20 minutes. Subsequently, 10 µL of 1 M NaBH<sub>3</sub>CN was added to each reaction, and the tubes were incubated at room temperature overnight. The AMAC-labeled disaccharides were separated by RP-HPLC in duplicate/triplicate using a Zorbax Eclipse XDB-C18 RP-HPLC column (3.5 µm, 2.1 × 150 mm; Agilent Technologies, Stockport, UK), as described previously.<sup>43,44</sup> Disaccharide types were identified/quantitated in comparison with AMAC-labeled commercial disaccharide standards (Iduron). The experiments were performed in four batches (each containing young and old donors), which were run on separate days.

Integration analysis of peak areas enabled relative quantification of HS disaccharides and HS composition. The following AMAC-labeling disaccharide correction factors were determined following labeling of known amounts of disaccharide standards (according to the method described by Deakin and Lyon<sup>44</sup>) and used for relative quantification: UA2S-GlcNS6S, 1.29; UA-GlcNS(6S), 1.19; UA(2S)-GlcNS, 1.0; UA-GlcNS, 1.12; UA-GlcNAc(6S), 1.11; UA-GlcNAc, 1.04. Each component of HS composition was compared between young and old donors by 2-tailed Student's *t*-test after logit transformation to correct for the ratiometric and compositional nature of the data.<sup>45</sup> Total HS quantity values were obtained for each sample by summing the quantity values of the individual HS disaccharides for that sample from the compositional analysis. The total HS quantity values underwent logarithmic transformation before statistical analysis to stabilize variance.<sup>46,47</sup> A 2-way ANOVA was applied to test for significant differences between the donor age groups while controlling for the batch effect. A likelihood ratio of the ANOVA model with and without interaction showed no significant batch-age group interaction. Since the model without interaction explained the data better (the Akaike information criterion was lower), statistical testing was done by performing 2-way ANOVA with Type II sum of squares on the reduced model (i.e., without interaction). In addition, since the BrM and NSR samples for each donor always were in the same batch, the ratio between them was not subject to batch effect. Therefore, testing for a difference in this ratio between

donor age groups could be performed with a 2-tailed Student's *t*-test.

### Preparation of Tissue Sections for Immunofluorescence Microscopy

As above, donor eyes were obtained from the Manchester Eye Bank, all without known retinal disease or visual impairment (see Supplementary Table S2 for ages and other details).

Donor eyes were fixed in 4% (vol/vol) formaldehyde for two hours at room temperature, as described previously.<sup>22,32,34</sup> Briefly, the macular region was removed using a 5-mm biopsy punch (SCHUCO International, London, UK) and further fixed in 4% (vol/vol) formaldehyde for 16 hours at 4°C. Each sample was set in OCT cryoprotectant (RA Lamb, Eastbourne, UK); 5- $\mu$ m tissue slices were made using a Leica CM1850 cryostat and these were mounted on poly-L-lysine coated microscope slides (Menzel-Gläser, Saarbrückene, Germany). Slides were stored at -80°C before immunohistochemical analysis.

### Immunolocalization of HS and Heparanase-1 in Human Macula

Immunohistochemistry experiments for HS were performed by application of monoclonal antibodies specific for HS (10E4 and 3G10), in association with fluorescently labeled secondary antibodies, to human eye sections, as described previously.<sup>34</sup> The 10E4 monoclonal antibody recognizes a common N-sulfated epitope within HS, while the 3G10 monoclonal antibody recognizes HS stubs after digestion with heparinase III.<sup>48</sup> Therefore, together, they may be used to determine the overall distribution of HS in tissues. Heparanase-1 was detected using polyclonal antibody 733.<sup>49</sup>

Before staining, microscope slides were incubated with chilled (-20°C) histological grade acetone (Sigma, Poole, UK) for 20 seconds before being washed thoroughly in PBS. Squares were drawn round each tissue section using a hydrophobic barrier pen (VectaLabs, Peterborough, UK) to prevent treatment contamination from adjacent sections. Pretreatment with heparinase III (10  $\mu$ U/mL in PBS at 37°C for 2 hours; Iduron) was done before staining with 3G10. The tissue sections then were blocked by incubation at room temperature for 1 hour with PBS containing 1 mg/mL BSA, 1% (vol/vol) goat serum and 0.1% (vol/vol) Triton X-100.

For each experiment, the relevant antibody was diluted 1:100, applied to tissue sections (100  $\mu$ L/section), and incubated for 16 hours at 4°C. After extensive washing with PBS, goat anti-mouse IgG/IgM (or goat anti-rabbit IgG for heparanase-1 staining) AlexaFluor488-conjugated secondary antibody (Invitrogen, Paisley, UK), diluted 1:100 in PBS, was added to each tissue section for 2 hours at room temperature. Finally, 4',6-diamidino-2-phenylindole (DAPI) was applied as a nuclear counterstain (at 0.5  $\mu$ g/mL in PBS for 10 minutes) before mounting with Vectashield medium and application of a coverslip. Control experiments were conducted where tissue sections were treated with blocking buffer instead of primary antibody, and where heparinase III digestion was omitted before 3G10 staining.

### Relative Binding of CFH CCP6-8 402H and 402Y Variants to BrM

Recombinant proteins representing the AMD-associated polymorphic region of CFH (comprising CCP domains 6-8) were made for 402H and 402Y variants, as described previously.<sup>24</sup> Both proteins were labeled equally with different fluorophores, and equimolar amounts of both proteins were mixed

together and applied exogenously to human eye tissue sections, where their relative fluorescent intensities on BrM were determined and analyzed as described previously.<sup>22</sup> Staining was performed on five donors in their 30s and five donors in their 80s (for details see Supplementary Table S3). For each age group, the fluorescent intensity values obtained were normalized using the 402Y variant signal, and then represented as percentage binding.

### Image Capture and Data Analysis

Images were collected on an Olympus BX51 upright microscope using a  $\times 10/0.30$  Plan FlN objective and captured using a Coolsnap ES camera (Photometrics, Maidenhead, UK) operated with MetaVue Software (v6.1; Molecular Devices, Sunnyvale, CA, USA), using specific band pass filter sets for FITC and DAPI, as described previously.<sup>32,34</sup> Images were analyzed using ImageJ64 (v1.40g; available in the public domain at <http://rsb.info.nih.gov/ij>).

Relative quantification of HS and heparanase-1 in BrM of young versus old donors was determined as described below; the experiment was performed blind with respect to the age of the donor tissue. The same technique was used for exogenously applied 402H and 402Y variants of CFH CCP6-8 domains. Grayscale images of macular BrM were analyzed with ImageJ for each donor (one test section and one control section). For each section, three areas were selected at random locations (i.e., left, middle, and right) along the full length of BrM imaged, each of length 100  $\mu$ m (as demonstrated in Supplementary Fig. S1). In each area, a polygon was drawn around BrM. ImageJ then was used to calculate the mean fluorescence per unit area within the polygon, and the area enclosed. These were multiplied to obtain a value representing the total quantity of fluorescence for a standardized (100  $\mu$ m) length of BrM (i.e., independent of differences in membrane thickness between donors). The mean control signal then was subtracted from the mean test signal. Statistical analysis was performed using 2-tailed Student's *t*-test after logarithmic transformation.

## RESULTS

### Analysis of HS Disaccharides in BrM and NSR by RP-HPLC

The BrM and NSR samples were obtained and pooled from both retinas of individual human donors of differing age. The GAGs were extracted and purified separately for each tissue sample, and the HS chains digested into disaccharides using bacterial heparinase enzymes. Disaccharides were labeled with AMAC (a fluorescent dye) and analyzed using single-step RP-HPLC, leading to the detection of six major HS disaccharides in BrM and NSR samples.<sup>43,44</sup> Integration analysis of peak areas enabled quantification of these disaccharides relative to standards, and the total HS quantity of each sample was obtained by summing the values of the six constituent HS disaccharides.<sup>43,44</sup>

Figure 1A shows the composition of HS from BrM in young versus old donors, along with the percentages of N-sulfated, 6-O-sulfated, and 2-O-sulfated disaccharides determined from the six disaccharides. The proportion of the UA(2S)-GlcNS disaccharide (i.e., 2-sulfated uronic acid with N-sulfated glucosamine) was significantly lower in old versus young donors ( $P = 0.021$ ). By contrast, the proportion of the completely unsulfated UA-GlcNAc disaccharide (uronic acid with N-acetylglucosamine) was significantly higher in the old donor tissues ( $P = 0.017$ ); the other four disaccharides, while

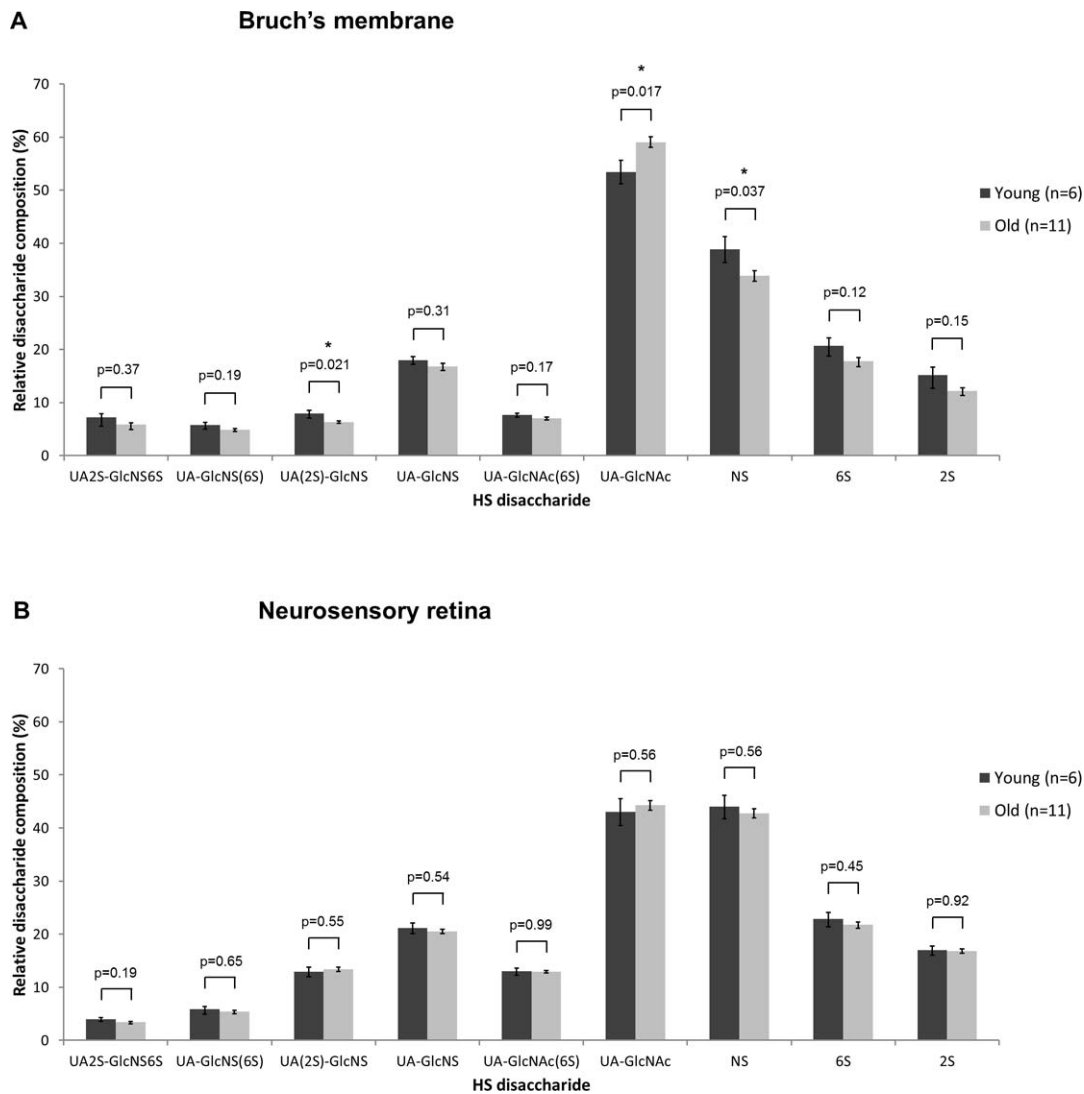


**FIGURE 1.** Compositional analysis of HS disaccharides by RP-HPLC comparing tissue from young versus old donors: (A) BrM, (B) NSR. Results are shown for each age group as mean total percentages ( $\pm$  SEM) for each of the six HS disaccharides analyzed. In addition, the mean total percentage proportions of N-sulfated (NS), 6-O-sulfated (6S), and 2-O-sulfated (2S) HS disaccharides are shown. Statistical significance was determined, for the comparison of HS from young versus old donor tissues, by Student's *t*-test after logit transformation; \**P* < 0.05.

all being at slightly lower levels in the BrM from old donors, were not statistically significant. Overall, the mean proportions of N-sulfated, 6-O-sulfated, and 2-O-sulfated HS disaccharides were lower in BrM from old compared to young donors (Fig. 1A); this difference was significant for N-sulfated disaccharides ( $P = 0.037$ ), but did not reach statistical significance for 6-O-sulfated ( $P = 0.12$ ) or 2-O-sulfated disaccharides ( $P = 0.15$ ). Taken together these results indicated that HS sulfation in BrM decreases slightly with age.

For HS from the NSR, the degree of sulfation (Fig. 1B) generally was higher than HS from BrM, including the proportions of N-sulfated, 6-O-sulfated, and 2-O-sulfated HS disaccharides. In contrast to the results for BrM, the degree of HS sulfation was very similar in both age groups; that is, no age-related alteration in HS sulfation in the NSR was observed.

Substantial changes were seen in the total quantity of HS from young versus old BrM, whereas there was no age-related change in the amount of HS in NSR. For example, the ratio of HS in BrM to that in NSR was significantly lower in the old compared to the young age group ( $P = 0.024$ , Fig. 2). Furthermore, the quantity of HS in BrM was on average

49.7% lower ( $P = 0.006$ , Fig. 3) in the old compared to the young donor tissue; no such reduction in HS was seen in the NSR ( $P = 0.57$ ). Hence, we have identified a significant and substantial age-related decrease in the amount of HS in BrM, with a 50% lower level in old versus young donors (mean ages of 82 and 32 years, respectively).

### Analysis of HS in Macular BrM by Immunohistochemistry

In the above experiments, the entire BrM was analyzed (pooled from two eyes) to provide sufficient tissue for disaccharide analysis. Therefore, to determine whether age-related changes in HS occur within BrM from the macular region alone, immunolocalization of HS using 10E4 and 3G10 antibodies was done using the methodology we have described previously.<sup>3,4</sup> The quantity of HS immunolabeling was calculated, adjusting for the thickness of BrM, since this is known to vary with age.<sup>50-52</sup> As demonstrated by the representative images in Figures 4B and 5B, the degree of HS immunofluorescence in BrM is more intense in the young compared to the old donor

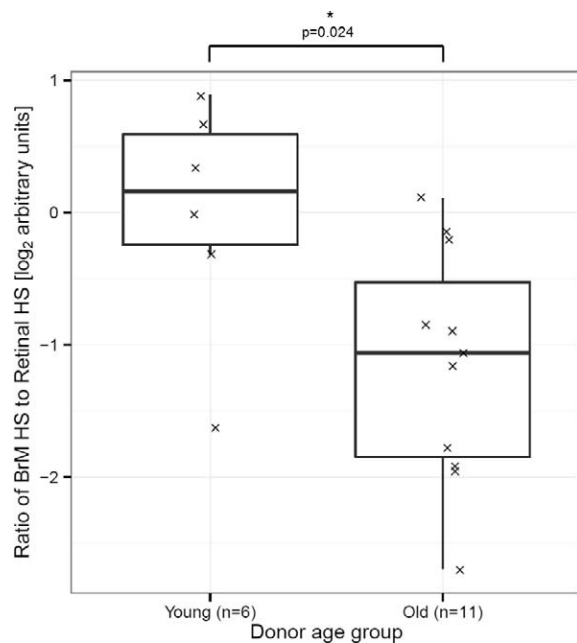


**FIGURE 2.** Box plot showing the ratio of HS quantity in BrM relative to NSR (*Retinal*) in young versus old donors. Results are shown for each age group as the median (*bold horizontal line*), first and third quartiles (*box*), 95% quintiles (*whiskers*), together with the raw data-points (*crosses*). Data are presented on the logarithmic scale. The ratio was significantly lower in the old age group (Student's *t*-test,  $P = 0.024$ ).

sections (i.e., for the 10E4 and 3G10 antibodies). In the case of 10E4 (Fig. 4B), this gave a localization pattern that essentially was identical to that which we have reported previously in old donor tissues (59–82 years)<sup>34</sup>; that is, with strong (relative) staining in the RPE and BrM, and moderate staining in the choroidal stroma and blood vessel walls. While less intense, 3G10 gave a similar pattern of staining (Fig. 5B) compared to 10E4. Quantitation of the HS staining in the BrM from six old and five young donors (see Supplementary Table S2) revealed that the mean level of HS in macular BrM was 61% ( $P = 0.02$ ) or 48% ( $P = 0.03$ ) lower in the old compared to young donors; that is, using 10E4 (Fig. 4A) and 3G10 (Fig. 5A) antibodies, respectively.

#### Analysis of Heparanase-1 in Macular BrM

The age-related reduction of HS in human BrM (described above) could be due to the loss of HS itself through increased enzymatic degradation with age (e.g., by heparanase-1<sup>53</sup>). Thus, immunofluorescent microscopy was done to compare the level of heparanase-1 in young and old macular tissue (five and seven donors, respectively; see Supplementary Table S4). Heparanase-1 staining was present in the BrM of all donor macular tissues (see Fig. 6B for representative images). However, while the degree of immunolabeling was on average 24% higher in old donors, this was not statistically significant ( $P = 0.56$ , Fig. 6A).

#### The Binding of Exogenously Applied CFH CCP6-8 402H and 402Y Variants to Macular BrM

As observed previously, in older donor tissue, the disease-associated 402H form of CFH bound significantly less well to BrM (Fig. 7).<sup>22</sup> However, when repeated using younger donor material, the difference between the binding levels of the two

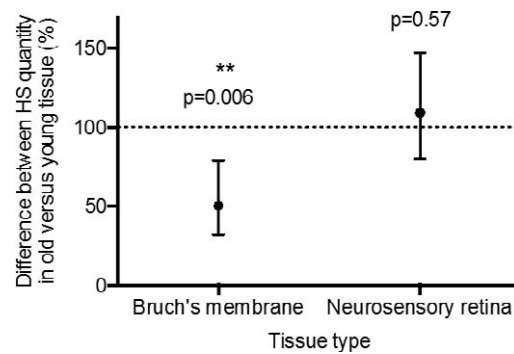


**FIGURE 3.** Plot showing the mean percentage difference in HS quantity between young and old donors for BrM and NSR. Results are shown as mean and 95% confidence interval following statistical testing by 2-way ANOVA. For BrM, the quantity of HS was 50% lower in old donors ( $P = 0.006$ );  $**P < 0.01$ .

variants was significantly smaller ( $P = 0.019$ , Fig. 7), indicating that the observed effect of the AMD-associated Y402H polymorphism in this region of CFH becomes more pronounced with age.

## DISCUSSION

In this study, we used a highly sensitive labeling method in conjunction with RP-HPLC to investigate changes with age in the composition and quantity of HS in human BrM, as well as in the NSR for comparison. This showed that the amount of HS in BrM (but not NSR) decreases significantly and substantially with age, by approximately 50% between samples with mean ages of 32 and 82 years. This is accompanied by a small but significant change in HS composition, with a reduction in the degree of sulfation; while the HS in the NSR was significantly more sulfated than that in the BrM, there was no age-related change in HS composition in this tissue. The immunohistochemical analyses also demonstrated that the quantity of HS in human BrM decreases with age, and that this occurs within the macular region.

The strengths of this study include the use of a validated, highly sensitive, method of HS detection alongside reference standards.<sup>43,44</sup> This enabled us to analyze potential changes in HS quantity/composition at the level of individual human donors, rather than reporting on pooled tissue from several individuals; each sample was run in duplicate or triplicate, and the results were analyzed while blinded to donor age or tissue type. Hence, we have been able to observe the degree of interindividual variation in HS levels; we had expected to see some heterogeneity; for example, due to biological variation, differences in postmortem time, cause of death, and so forth. However, from the data on BrM and NSR, it can be seen that there is remarkable consistency between the HS prepared from different donors, for example with highly similar compositions and small errors, at least for the disaccharides analyzed here (Fig. 1B). Analysis of isolated BrM represents an improvement over previous studies (e.g., of macular homogenates<sup>54</sup>). This has revealed clearly that age is the major variable affecting the composition/quantity of HS within BrM. However, the limits of detection by RP-HPLC meant that we had to use tissue from the whole retina (pooled from both eyes from a particular donor), rather than the macula only. Another limitation with the RP-HPLC approach is that results are presented as a global mean of sulfation at the level of HS disaccharides; hence, some differences in regional sulfation patterns between young and old donors might be missed. For this reason, and to provide

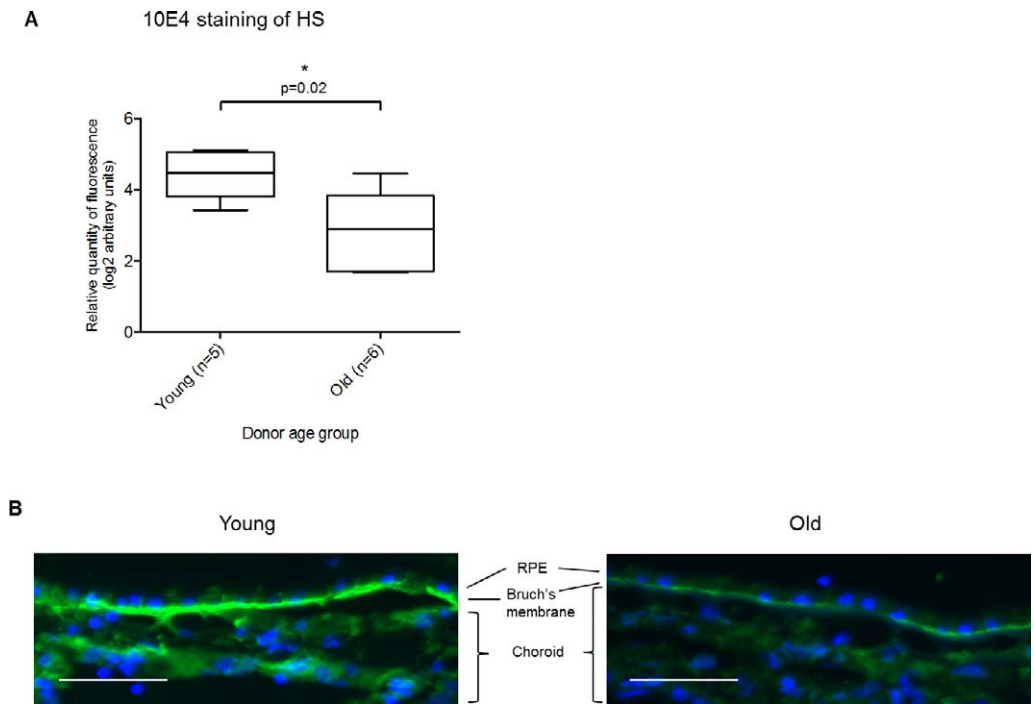


**FIGURE 4.** Immunolocalization and quantification of HS in macular BrM from young versus old donors, using 10E4 monoclonal antibody. **(A)** Quantification of 10E4 staining in BrM; the median (*horizontal line*), first and third quartiles (*box*), and 95% quintiles (*whiskers*) are shown; statistical significance was determined using Student's *t*-test (\* =  $P < 0.05$ ). **(B)** Representative images of HS staining by 10E4 (*green staining*) in young (M15468, 18 years) and old (M15721, 89 years) donors. *Blue staining* represents nuclear labeling by DAPI, and the *scale bar* indicates 50  $\mu\text{m}$ .

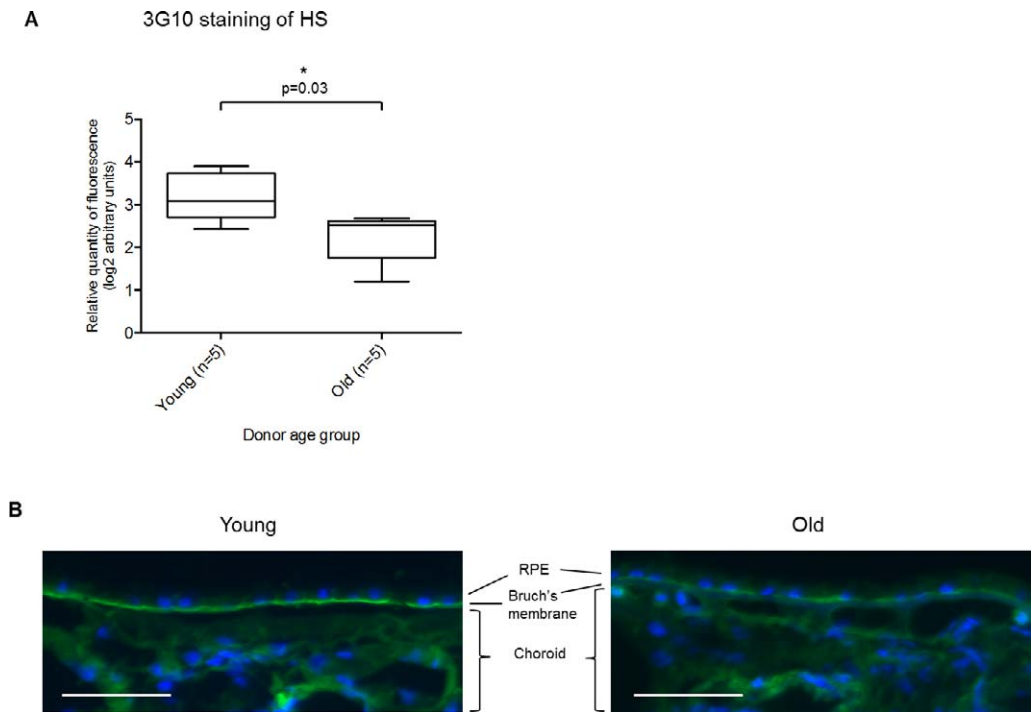


**FIGURE 5.** Immunolocalization and quantification of HS in macular BrM from young versus old donors, using 3G10 monoclonal antibody following heparinase III digestion. **(A)** Quantification of 3G10 staining in BrM; the median (*horizontal line*), first and third quartiles (*box*), and 95% quintiles (*whiskers*) are shown; statistical significance was determined using Student's *t*-test (\* $P < 0.05$ ). **(B)** Representative images of HS staining by 3G10 (*green staining*) in young (M15468, 18 years) and old (M15721, 89 years) donors. *Blue staining* represents nuclear labeling by DAPI, and the *scale bar* indicates 50  $\mu\text{m}$ .

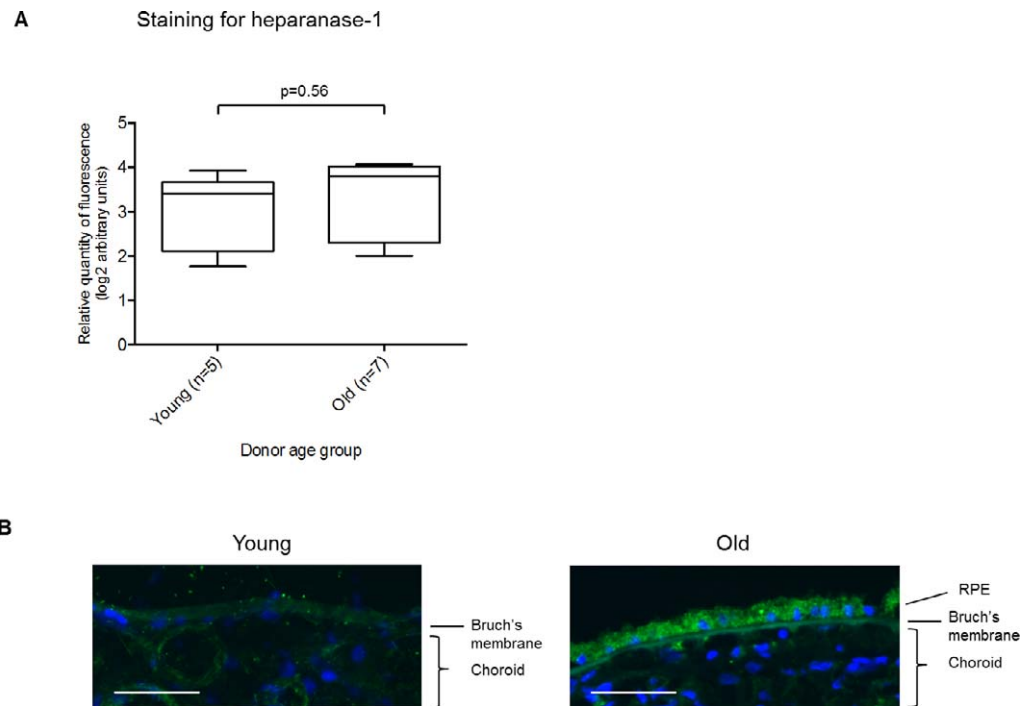


**FIGURE 6.** Immunolocalization and quantification of heparanase-1 in macular BrM from young versus old donors, using polyclonal antibody 733. **(A)** Quantification of heparanase-1 staining in BrM; the median (*horizontal line*), first and third quartiles (*box*), and 95% quintiles (*whiskers*) are shown; statistical significance was determined using Student's *t*-test ( $P=0.56$ ). **(B)** Representative images of heparanase-1 staining (*green staining*) in young (M14209, 35 years) and old (M11913, 79 years) donors. *Blue staining* is labelling by DAPI; *scale bars*: 50  $\mu$ m.

additional “structural” information, we also performed immunofluorescence microscopy for HS in human macular sections, though we acknowledge that immunofluorescence is not always proportional to the amount of antigen. However, immunofluorescence was performed using two separate antibodies and in a standardized manner (e.g., same microscope settings used for all imaging and imaging performed at one sitting for all donors in each experiment) to maximize confidence in this approach.

Previous studies have demonstrated tissue-specific differences in HS structure.<sup>55–58</sup> Here, we have seen that such variations can occur within two tissues that are closely positioned (i.e., in the BrM and NSR); this is consistent with the differential distribution of GAG epitopes present within these regions of the human eye that we mapped using phage-display antibodies.<sup>34</sup> There also is evidence that HS in particular tissues may undergo gradual changes with age. For example, Feyzi et al.<sup>57</sup> observed that there is a progressive increase in 6-O-sulfation in the HS in human aorta over several decades, accompanied by increased binding to platelet-derived growth factors. More recently, another study<sup>58</sup> demonstrated an age-related decrease in the proportion of the HS disaccharide UA(2S)-GlcNS(6S) on the surface of human outgrowth endothelial cells, which correlated with a decline in their migratory response toward VEGF. In the case of the human eye, our work suggested that two nearby tissues (i.e., BrM and the NSR) differ significantly in HS sulfation (perhaps reflecting differences in their developmental origins, cellular contents, and functions), and that BrM undergoes an age-related loss in HS quantity and sulfation, whereas the NSR does not.

This is the first study (to our knowledge) that has investigated systematically whether changes in HS occur in human BrM with age. The observation of an age-related reduction in HS quantity and sulfation within BrM has important implications for our understanding of AMD patho-

genesis. As described previously, HS is a major binding partner of CFH in human macular BrM,<sup>22,23</sup> and the 402H form of CFH requires a high degree of HS sulfation for binding.<sup>22,24,25</sup> Thus, the presence of less HS and its decreased sulfation in older BrM

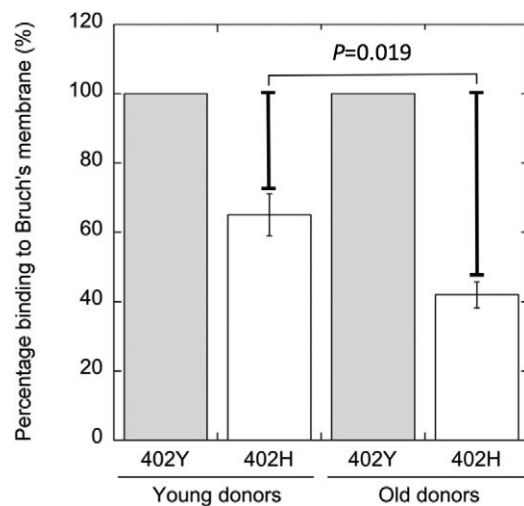


**FIGURE 7.** Poor binding of the 402H form of CFH to BrM becomes more pronounced with age. Fluorescently labeled CCP6-8 proteins (402Y and 402H forms) were applied exogenously to five younger donors (*left hand side*) and five older donors (*right hand side*). In each case, the percentage binding values for the disease-associated 402H form to BrM are shown, each normalized to their respective 402Y variant signal (i.e., young or old). The ratio of binding between the 402Y and 402H proteins was calculated for each donor set (young and old), log2 transformed, and statistical significance was determined using Student's *t*-test, where  $P < 0.05$  was determined to be significant. The 402H data are shown  $\pm$  SEM;  $n = 5$ .

means that fewer binding sites are likely to be available for CFH, particularly for the 402H variant, which appears to interact with rather rare sequences.<sup>24</sup>

The HSPGs in mammalian tissues are thought to undergo synthesis/turnover in a regulated manner.<sup>53</sup> Following proteoglycan core protein expression, HS chains are elongated by proteins from the EXT family and sulfate groups are added by sulfotransferase enzymes; this all occurs within the Golgi apparatus. In the extracellular environment, sulfates can be removed by endosulfatases and HS chains may be broken down by heparanase-1.<sup>53</sup> Hence, potential mechanisms for an age-related decrease in HS (and HS sulfation) may include decreased biosynthesis of HSPGs, reduced HS chain length, increased sulfatase activity, increased HS breakdown by heparanase-1, or increased proteolytic degradation of a PG core protein(s). We observed that the degree of reduction in 10E4 and 3G10 staining for HS was approximately similar (61%,  $P = 0.02$  and 48%,  $P = 0.03$ , respectively), suggesting that HS chain length may remain relatively constant (or decrease only slightly) with age, and that HS chain degradation does not explain the loss of HS from BrM with age. In addition, there was no significant change in the proportion of 6-O-sulfated HS with age, arguing against a role for increased sulfatase activity (unless this was balanced by changes in 6-O-sulfotransferase activity). Therefore, the most likely explanation is decreased synthesis or increased breakdown of HS core proteins. Indeed, preliminary experiments suggest a reduction in HSPGs in BrM, including perlecan (data not shown). This would seem to coincide with a recent proteomic study of mouse BrM/choroid, which observed a 56% decrease in the level of perlecan in wild type mice from age 8 to 24 months.<sup>59</sup>

The results observed here could explain the age-dependence of AMD; that is, why even those individuals with the highest genetic and environmental risk factors do not develop clinical disease for many decades of life. This would be because, while HS levels are "high" in the first several decades of life, CFH (even the 402H form) could still bind to macular BrM in quantities sufficient to prevent complement activation. However, as HS levels in BrM decrease over subsequent decades, a threshold may be reached where CFH is unable to bind in quantities sufficient to prevent complement activation/amplification; this threshold might be reached more quickly in the presence of the 402H variant, because of its restricted specificity for HS and consequently the rarity of its binding sites.<sup>22,24</sup> This hypothesis is supported by previous studies demonstrating increased complement activation in human BrM/choroid with age<sup>20</sup> and in 402H homozygotes.<sup>21</sup>

One previous study reported that HS (either from human BrM/choroid or from bovine kidney) enhances CFH's cofactor activity for factor I-mediated cleavage of C3b; that is, HS increases the inhibition of the activation/amplification of the alternative pathway of complement.<sup>60</sup> In this context, an age-related reduction in HS levels would mean a progressive impairment of complement regulation in BrM. As above, a threshold might be reached at a particular age (depending on genetic background and environmental risk factors) where reduced HS would lead to complement overactivation, and thereby contribute to the progression to AMD. Thus, we hypothesize that AMD could arise through the combination of a permissive genotype (i.e., the Y402H polymorphism, which alters the HS-recognition properties of the CFH protein) along with age-related changes in HS structure within BrM, that together would lead to a decrease in CFH binding and impaired regulation of complement.

In conclusion, this study provided a systematic analysis of age-related changes in HS quantity/composition in human BrM and the NSR. This demonstrates that HS levels in BrM decrease significantly and substantially with age (in the whole retina and

in the macula), and that HS sulfation levels also decrease to some degree. In combination with our previous work on HS-CFH interactions, this may have important implications for our understanding of AMD pathogenesis and potential therapeutic approaches.

### Acknowledgments

The authors thank Isaac Zambrano, PhD (Manchester Eye Bank, Manchester Royal Eye Hospital, and Manchester Biomedical Research Centre, Manchester, UK), for assistance with obtaining the donor eye tissue used in this study. The anti-heparanase antibody 733 was kindly provided by Israel Vlodavsky, PhD (Rappaport Faculty of Medicine, Technion, Haifa, Israel).

Supported by the Medical Research Council (Grants G0900592, K004441, G0701165 and G0902170), and the NIHR Manchester Biomedical Research Centre. The Bioimaging Facility microscopes used in this report were purchased with support from the BBSRC, Wellcome Trust and the University of Manchester Strategic Fund. TDLK is a recipient of a Fight for Sight Clinical Fellowship (1866). SJC is the recipient of an MRC Career Development Award (MR/K024418/1).

Disclosure: **T.D.L. Keenan**, None; **C.E. Pickford**, None; **R.J. Holley**, None; **S.J. Clark**, None; **W. Lin**, None; **A.W. Dowsey**, None; **C.L. Merry**, None; **A.J. Day**, None; **P.N. Bishop**, None

### References

- Congdon N, O'Colmain B, Klaver CC, et al. Causes and prevalence of visual impairment among adults in the United States. *Arch Ophthalmol*. 2004;122:477-485.
- Bunce C, Wormald R. Causes of blind certifications in England and Wales: April 1999-March 2000. *Eye (Lond)*. 2008;22:905-911.
- Day AJ, Clark SJ, Bishop PN. Understanding the molecular basis of age-related macular degeneration and how the identification of new mechanisms may aid the development of novel therapies. *Exp Rev Ophthalmol*. 2011;6:123-128.
- Anderson DH, Radeke MJ, Gallo NB, et al. The pivotal role of the complement system in aging and age-related macular degeneration: hypothesis re-visited. *Prog Retin Eye Res*. 2010;29:95-112.
- Langford-Smith A, Keenan TD, Clark SJ, Bishop PN, Day AJ. The role of complement in age-related macular degeneration: heparan sulphate, a ZIP code for complement factor H. *J Innate Immun*. 2014;6:407-416.
- Hageman GS, Anderson DH, Johnson LV, et al. A common haplotype in the complement regulatory gene factor H (HF1/CFH) predisposes individuals to age-related macular degeneration. *Proc Natl Acad Sci U S A*. 2005;102:7227-7232.
- Edwards AO, Ritter R III, Abel KJ, et al. Complement factor H polymorphism and age-related macular degeneration. *Science*. 2005;308:421-424.
- Klein RJ, Zeiss C, Chew EY, et al. Complement factor H polymorphism in age-related macular degeneration. *Science*. 2005;308:385-389.
- Haines JL, Hauser MA, Schmidt S, et al. Complement factor H variant increases the risk of age-related macular degeneration. *Science*. 2005;308:419-421.
- Hageman GS, Hancox LS, Taiber AJ, et al. Extended haplotypes in the complement factor H (CFH) and CFH-related (CFHR) family of genes protect against age-related macular degeneration: characterization, ethnic distribution and evolutionary implications. *Ann Med*. 2006;38:592-604.
- Fritsche LG, Chen W, Schu M, et al. Seven new loci associated with age-related macular degeneration. *Nat Genet*. 2013;45:433-439.



12. Seddon JM, Yu Y, Miller EC, et al. Rare variants in CFI, C3 and C9 are associated with high risk of advanced age-related macular degeneration. *Nat Genet.* 2013;45:1366-1370.
13. Sofat R, Casas JP, Webster AR, et al. Complement factor H genetic variant and age-related macular degeneration: effect size, modifiers and relationship to disease subtype. *Int J Epidemiol.* 2012;41:250-262.
14. Hageman GS, Luthert PJ, Victor Chong NH, et al. An integrated hypothesis that considers drusen as biomarkers of immune-mediated processes at the RPE-Bruch's membrane interface in aging and age-related macular degeneration. *Prog Retin Eye Res.* 2001;20:705-732.
15. Crabb JW, Miyagi M, Gu X, et al. Drusen proteome analysis: an approach to the etiology of age-related macular degeneration. *Proc Natl Acad Sci U S A.* 2002;99:14682-14687.
16. Donoso LA, Kim D, Frost A, Callahan A, Hageman G. The role of inflammation in the pathogenesis of age-related macular degeneration. *Surv Ophthalmol.* 2006;51:137-152.
17. Skeie JM, Fingert JH, Russell SR, Stone EM, Mullins RF. Complement component C5a activates ICAM-1 expression on human choroidal endothelial cells. *Invest Ophthalmol Vis Sci.* 2010;51:5336-5342.
18. Gerl VB, Bohl J, Pitz S, et al. Extensive deposits of complement C3d and C5b-9 in the choriocapillaris of eyes of patients with diabetic retinopathy. *Invest Ophthalmol Vis Sci.* 2002;43:1104-1108.
19. Mullins RF, Johnson MN, Faidley EA, Skeie JM, Huang J. Choriocapillaris vascular dropout related to density of drusen in human eyes with early age-related macular degeneration. *Invest Ophthalmol Vis Sci.* 2011;52:1606-1612.
20. Seth A, Cui J, To E, Kwee M, Matsubara J. Complement-associated deposits in the human retina. *Invest Ophthalmol Vis Sci.* 2008;49:743-750.
21. Mullins RF, Dewald AD, Streb LM, et al. Elevated membrane attack complex in human choroid with high risk complement factor H genotypes. *Exp Eye Res.* 2011;93:565-567.
22. Clark SJ, Perveen R, Hakobyan S, et al. Impaired binding of the age-related macular degeneration-associated complement factor H 402H allotype to Bruch's membrane in human retina. *J Biol Chem.* 2010;285:30192-30202.
23. Clark SJ, Ridge LA, Herbert AP, et al. Tissue-specific host recognition by complement factor H is mediated by differential activities of its glycosaminoglycan-binding regions. *J Immunol.* 2013;190:2049-2057.
24. Clark SJ, Higman VA, Mulloy B, et al. His-384 allotypic variant of factor H associated with age-related macular degeneration has different heparin binding properties from the non-disease-associated form. *J Biol Chem.* 2006;281:24713-24720.
25. Prosser BE, Johnson S, Roversi P, et al. Structural basis for complement factor H linked age-related macular degeneration. *J Exp Med.* 2007;204:2277-2283.
26. Mullins, RF, Sohn EH. Bruch's membrane: the critical boundary in macular degeneration. In: Yind DG-S, ed. *Age Related Macular Degeneration - The Recent Advances in Basic Research and Clinical Care.* Rijeka, Croatia: InTech; 2012.
27. Booij JC, Baas DC, Beisekeeva J, Gorgels TG, Bergen AA. The dynamic nature of Bruch's membrane. *Prog Retin Eye Res.* 2010;29:1-18.
28. Clark SJ, Bishop PN, Day AJ. Complement factor H and age-related macular degeneration: the role of glycosaminoglycan recognition in disease pathology. *Biochem Soc Trans.* 2010;38:1342-1348.
29. Kreuger J, Kjellen L. Heparan sulfate biosynthesis: regulation and variability. *J Histochem Cytochem.* 2012;60:898-907.
30. Schaefer L, Schaefer RM. Proteoglycans: from structural compounds to signaling molecules. *Cell Tissue Res.* 2010;339:237-246.
31. Theocharis AD, Skandalis SS, Tzanakakis GN, Karamanos NK. Proteoglycans in health and disease: novel roles for proteoglycans in malignancy and their pharmacological targeting. *FEBS J.* 2010;277:3904-3923.
32. Keenan TD, Clark SJ, Unwin RD, et al. Mapping the differential distribution of proteoglycan core proteins in the adult human retina, choroid, and sclera. *Invest Ophthalmol Vis Sci.* 2012;53:7528-7538.
33. Lindahl U, Li JP. Interactions between heparan sulfate and proteins-design and functional implications. *Int Rev Cell Mol Biol.* 2009;276:105-159.
34. Clark SJ, Keenan TD, Fielder HL, et al. Mapping the differential distribution of glycosaminoglycans in the adult human retina, choroid, and sclera. *Invest Ophthalmol Vis Sci.* 2011;52:6511-6521.
35. Sarrazin S, Lamanna WC, Esko JD. Heparan sulfate proteoglycans. *Cold Spring Harb Perspect Biol.* 2011;37:a004952.
36. Clark SJ, Bishop PN, Day AJ. The proteoglycan glycomatrix: a sugar microenvironment essential for complement regulation. *Front Immunol.* 2013;4:412.
37. Park PJ, Shukla D. Role of heparan sulfate in ocular diseases. *Exp Eye Res.* 2013;110:1-9.
38. Bruinsma IB, te Riet L, Gevers T, et al. Sulfation of heparan sulfate associated with amyloid-beta plaques in patients with Alzheimer's disease. *Acta Neuropathol.* 2010;119:211-220.
39. Ohno-Matsui K. Parallel findings in age-related macular degeneration and Alzheimer's disease. *Prog Retin Eye Res.* 2011;30:217-238.
40. Kaarniranta K, Salminen A, Haapasalo A, Soininen H, Hiltunen M. Age-related macular degeneration (AMD): Alzheimer's disease in the eye? *J Alzheimers Dis.* 2011;24:615-631.
41. Raman K, Kuberan B. Chemical tumor biology of heparan sulfate proteoglycans. *Curr Chem Biol.* 2010;4:20-31.
42. Blackhall FH, Merry CL, Davies EJ, Jayson GC. Heparan sulfate proteoglycans and cancer. *Br J Cancer.* 2001;85:1094-1098.
43. Holley RJ, Deligny A, Wei W, et al. Mucopolysaccharidosis type I, unique structure of accumulated heparan sulfate and increased N-sulfotransferase activity in mice lacking alpha-L-iduronidase. *J Biol Chem.* 2011;286:37515-37524.
44. Deakin JA, Lyon M. A simplified and sensitive fluorescent method for disaccharide analysis of both heparan sulfate and chondroitin/dermatan sulfates from biological samples. *Glycobiology.* 2008;18:483-491.
45. Filzmoser P, Hron K, Reimann C. Univariate statistical analysis of environmental (compositional) data: problems and possibilities. *Sci Total Environ.* 2009;407:6100-6108.
46. Bland JM, Altman DG. Transforming data. *BMJ.* 1996;312:770.
47. Feng C, Wang H, Lu N, Tu XM. Log transformation: application and interpretation in biomedical research. *Stat Med.* 2013;32:230-239.
48. David G, Bai XM, Van der Schueren B, Cassiman JJ, Van den Berghe H. Developmental changes in heparan sulfate expression: in situ detection with mAbs. *J Cell Biol.* 1992;119:961-975.
49. Zetser A, Levy-Adam F, Kaplan V, et al. Processing and activation of latent heparanase occurs in lysosomes. *J Cell Sci.* 2004;117:2249-2258.
50. Ramrattan RS, van der Schaft TL, Mooy CM, et al. Morphometric analysis of Bruch's membrane, the choriocapillaris, and the choroid in aging. *Invest Ophthalmol Vis Sci.* 1994;35:2857-2864.
51. Okubo A, Rosa RH Jr, Bunce CV, et al. The relationships of age changes in retinal pigment epithelium and Bruch's membrane. *Invest Ophthalmol Vis Sci.* 1999;40:443-449.
52. Karampelas M, Sim DA, Keane PA, et al. Evaluation of retinal pigment epithelium-Bruch's membrane complex thickness in

- dry age-related macular degeneration using optical coherence tomography. *Br J Ophthalmol*. 2013;97:1256-1261.
53. Li JP, Vlodavsky I. Heparin, heparan sulfate and heparanase in inflammatory reactions. *Thromb Haemost*. 2009;102:823-828.
54. Kliffen M, Mooy CM, Luidier TM, et al. Identification of glycosaminoglycans in age-related macular deposits. *Arch Ophthalmol*. 1996;114:1009-1014.
55. Lindahl B, Eriksson L, Lindahl U. Structure of heparan sulphate from human brain, with special regard to Alzheimer's disease. *Biochem J*. 1995;306:177-184.
56. Kato M, Wang H, Bernfield M, Gallagher JT, Turnbull JE. Cell surface syndecan-1 on distinct cell types differs in fine structure and ligand binding of its heparan sulfate chains. *J Biol Chem*. 1994;269:18881-18890.
57. Feyzi E, Saldeen T, Larsson E, Lindahl U, Salmivirta M. Age-dependent modulation of heparan sulfate structure and function. *J Biol Chem*. 1998;273:13395-13398.
58. Williamson KA, Hamilton A, Reynolds JA, et al. Age-related impairment of endothelial progenitor cell migration correlates with structural alterations of heparan sulfate proteoglycans. *Aging Cell*. 2013;12:139-147.
59. Garland DL, Fernandez-Godino R, Kaur I, et al. Mouse genetics and proteomic analyses demonstrate a critical role for complement in a model of DHRD/ML, an inherited macular degeneration. *Hum Mol Genet*. 2014;23:52-68.
60. Kelly U, Yu L, Kumar P, et al. Heparan sulfate, including that in Bruch's membrane, inhibits the complement alternative pathway: implications for age-related macular degeneration. *J Immunol*. 2010;185:5486-5494.